 doi:10.20944/preprints202211.0051.v1

Article

Comparing Rain Gauge and Weather Radar Data in the Estimation of the Pluviometric Inflow from the Apennine Ridge to the Adriatic Coast (Abruzzo Region - Central Italy)

Diego Di Curzio[1,2], Alessia Di Giovanni[1], Raffaele Lidori[3], Mario Montopoli[3,4] and Sergio Rusi[1, 3, *]

[1] Department of Engineering and Geology (InGeo), University "G. d'Annunzio" Chieti-Pescara, Italy; diego.dicurzio@unich.it (DDC); alessia.digiovanni@unich.it (ADG)
[2] Department of Water Management, Delft University of Technology, Netherland; D.DiCurzio@tudelft.nl
[3] Center of Excellence Telesensing of Environment and Model Prediction of Severe events, L'Aquila, Italy; raffaele.lidori@gmail.com (RL)
[4] National Research Council of Italy, Institute of Atmospheric Sciences and Climate (CNR-ISAC), Rome, Italy; m.montopoli@isac.cnr.it (MM)
* Correspondence: sergio.rusi@unich.it (RS)

Abstract: Accurate knowledge of the rain amount is an crucial driver in several hydro-meteorological applications. This is especially true in complex orography territories, which are typically impervious, thus leaving ungauged most of the mountain areas. Thanks to their spatial and temporal coverage, weather radars can potentially overcome such an issue. However, weather radar, if not accurately processed, can suffer from several limitations (e.g., beam blocking, altitude of the observation, path attenuation, indirectness of the measurement) that can hamper the reliability of the rain estimates performed. In this study, a comparison between rain gauge and weather radar retrievals is performed in the target area of the Abruzzo region in Italy, which is characterized by a heterogeneous orography ranging from the sea side to Apennine ridge. Consequently, the Abruzzo region has an inhomogeneous distribution of the rain gauges, with station density decreasing with the altitude reaching up to approximately 1500 m a.s.l. Notwithstanding, pluviometric inflow spatial distribution shows a sub-regional dependency as a function of four climatic and altimetric factors: coastal, hilly, mountain, and inner plain areas (i.e., Marsica). Such areas are used in this analysis to characterize the radar retrieval vs. rain gauge amounts in each of those zones. Compared to previous studies on the topic, the analysis presented an attention to the importance of an accurate selection of the climatic and altimetric sub-regional areas where undertake the radar vs. rain gauge comparison. This aspect is not only of great importance to correct biases in radar retrievals in a more selective way, but it also paves the way for more accurate hydro-meteorological applications (e.g., hydrological model initialization, quantify the aquifers recharge etc.) which, in general, require the accurate knowledge of rain amounts upstream of a basin. To fill the gap caused by the uneven rain gauge distribution, Ordinary Kriging has been applied on a regional scale to obtain 2D maps of rainfall data, which are cumulated on a monthly and yearly base. Weather radar data from the Italian mosaic are considered as well, in terms of rain rate retrievals and cumulations performed on the same time frame used for rain gauges. The period considered for the analysis is two continuous years: 2017 and 2018. The output of the elaborations are raster maps for both radar and interpolated rain gauges, where every pixel contains a rainfall quantity. Although the results show a general underestimation in the weather radar data especially in mountain and Marsica areas, even though within the 95% confidence interval of the OK estimation. Our analysis highlights that the average bias between radar and rain gauges, in terms of precipitation amounts, is a function of altitude and is almost constant in each of the selected areas. This achievement suggests that after a proper selection of homogeneous target areas, the radar retrievals can be corrected using the denser network of rain gauges typically distributed at lower altitudes and extend such correction at higher altitudes without loss of generality.

Keywords: rain gauge; weather radar rain retrievals; ordinary Kriging; water budget; Central Italy

 doi:10.20944/preprints202211.0051.v1

1. Introduction

The distribution of meteorological measurement stations on the Italian national territory is not homogeneous due to the logistical and morphological conditions of the mountain ranges. In particular, such distribution in the Apennine chain, where the study area is focused, is uneven and has a very poor coverage above 1000 m a.s.l. [1-3]. This becomes a critical issue especially when there is the need to have information of the water amount felt on mountain areas for example to estimate the recharge of aquifers [4].

On one hand, to overcome the issues related to a discrete and sparse distribution of rain gauges of the national and regional monitoring network, the spatial distribution of rainfall can be reconstructed using either traditional interpolation techniques [5-6], such Thiessen polygons, Triangulation with linear interpolation, Natural Neighbor, Inverse Weighted Distance, or Spline, or more advanced ones, like Geostatistics. This wide group of methods is based on the Regionalized Variable Theory [7], stating that values of a specific variable defined in space depend on each other [8-10]. According to this theory, measurements include a spatially correlated casual component, the mean value, and the residual non-systematic error [11]. These techniques are physically based, as they take advantage of the spatial variability structures of experimental measurements. In addition, they are implemented in a fashion that ensures optimal and unbiased prediction of the selected variables in areas where they are not measured.

On the other hand, weather RaDAR systems (Radio Detection And Ranging, hereafter named "radar" for simplicity) can represent an alternative solution, as they can provide a spatially seamless estimation of rainfall in near real-time. A single weather radar can cover large areas up to 200 km from the radar site with a time sampling of 5-10 min and a spatial range resolution from 125 m up to 500 m [12]. Weather radar estimates of near-surface precipitation can be affected by several limiting factors [13], which includes partial beam blocking from nearby orography, path attenuation caused by the liquid amount along the radar line of sighs, radiofrequency interferences and cone of silence, that is, unobserved areas close to the ground. Most of such issues can be reduced and compensated after proper processing of radar date [14] delivering filtered and reliable radar data. However, especially in complex orography, weather radar sites are often positioned on mountain peaks [15] to ensure large coverages and prevent mountain blocks with the unavoidable drawbacks of i) increasing the indirect character of the radar measurement in rain regimes caused by the increased distance between the radar measurement aloft and the surface level and ii) to likely have differences in the vertical distribution of hydrometeors (i.e. ice snow/ice is sampled by the radar aloft while liquid rain is falling below close to the surface) that makes the inversion of the radar acquisitions into rain rate more challenging. Several techniques exist to compensate for some of the radar limiting factors [16] although residual errors are difficult to be completely zeroed out.

Despite all the above-mentioned critical factors, weather radar-derived rainfall datasets are valuable with respect to rain gauge networks because they can potentially reduce the uncertainty about precipitation inflow volumes thanks to their higher spatial-temporal resolution. Weather radars are nowadays networked and generally used for weather surveillance, hydrological and meteorological purposes with special emphasis on data assimilation [17], in support to civil protection activities [18] as well as to better define the water budget in regional aquifers [19] or in wide catchment [20].

In the present study, the possibility of using an alternative precipitation evaluation technique based on weather radar surveys is analyzed. In particular, weather radar measurements from the Italian network have been compared to geostatistical estimations obtained through the application of the Ordinary Kriging (OK) methods to rain gauge measurements. Even though it is the most simplified geostatistical approach, if compared to more sophisticated techniques like Co-Kriging [21-24] or Kriging with External Drift [25-27], OK is not influenced by the uncertainty associated with auxiliary variables that are generally not quantified. For this reason, in this case, it has been considered appropriate,

Preprints (www.preprints.org) | NOT PEER-REVIEWED | Posted: 2 November 2022 doi:10.20944/preprints202211.0051.v1

as the main aim is to compare rainfall data collected by different sources and characterized by different supports.

The selected study area falls within the territory of the Abruzzo region and covers a portion of the Italian territory between the Adriatic coast and the Apennine chain.

Because of the complex elaboration of weather radar data, only two years (2017 and 2018) of annual and monthly datasets have been analyzed. For the comparison between the interpolated data from rain gauge network and the weather radar data, the Abruzzo territory has been divided in four homogeneous altimetric-climatic zones and the mean rainfall amount has been calculated for each one of them.

Moreover, a seasonal evaluation is elaborated: for every climatic zone, both sources of rainfall data are aggregated to a seasonal basis to highlight seasonal trends.

The manuscript first explains the study area and the used methods, then data are shown and discussed using maps and tables followed by conclusions.

2. Materials and Methods

2.1. Study area and datasets

The study area is represented by the whole Abruzzo Region with its heterogeneous territory. Its landscape includes mountain areas in the western part and more hilly and flat areas in the eastern (Figure 1); these different morphological features imply different meteorological and pluviometric conditions [28-29].

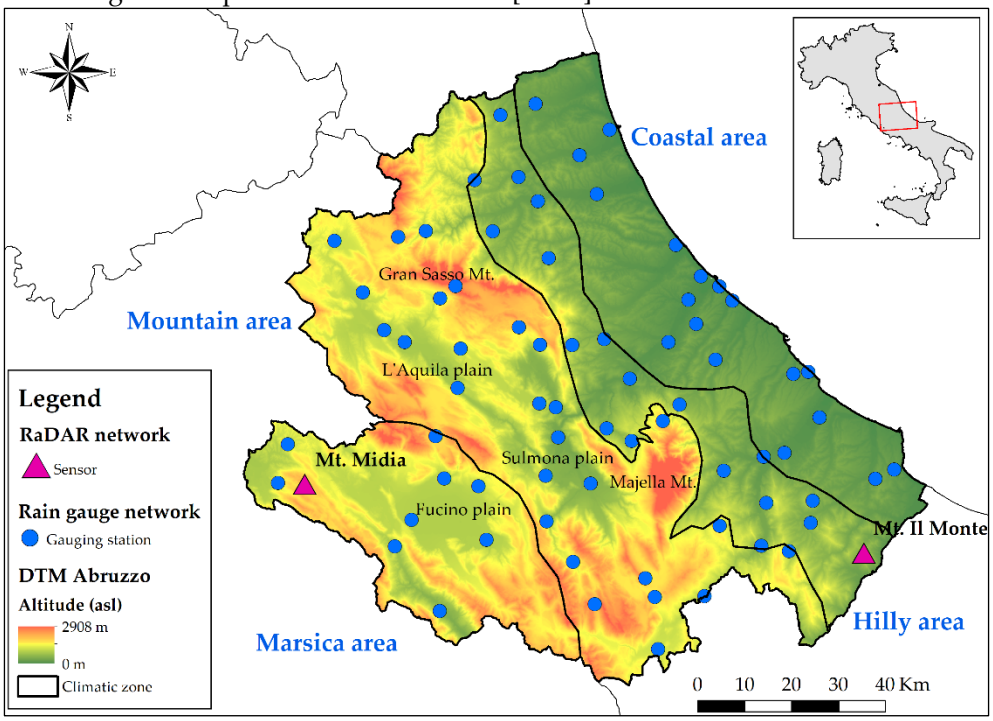

Figure 1. Study area divided in the four zones. Rain gauge and radar sensors are shown.

For these reasons, the study area has been divided into four zones based on different altitudes, climatic conditions, and morphological characteristics (Figure 1):

- coastal area, from sea level to about 300 m a.s.l., mainly includes the river plains and the seacoast land;
- hilly area, from about 300 to about 900 m a.s.l.; it comprises the hills behind the plains and the lower peaks;
- mountain area, from about 900 m to about 3000 m a.s.l., with drainage to the eastern side of the study area (Adriatic Sea) and includes the main peaks, usually corresponding to the major recharge area; in this area can be also find the Sulmona and L'Aquila plains;

Preprints (www.preprints.org) | NOT PEER-REVIEWED | Posted: 2 November 2022 doi:10.20944/preprints202211.0051.v1

- Marsica area, with drainage to the western side of the study area (Tyrrhenian Sea) which includes Fucino plain and nearby mountains.

This sub-division allows correlating precipitations to land features for more accurate data comparison.

Furthermore, considering each zone separately enables highlighting the differences inside the rain gauges' network: the coastal and hilly areas are the best covered, while the mountain and Marsica ones, show a consistent lack in the stations' distribution. As can be seen in Figure 1, automatic stations are mainly located in the flat areas (i.e., Fucino and Sulmona plains) leaving completely uncovered the peaks (i.e., Majella massif).

Table 1. Numbers of stations for every climatic zone used for Ordinary Kriging.

Climatic zone	Number of gauging stations
Coastal area	19
Hilly area	17
Mountain area	27
Marsica area	9

The annual and monthly rainfall datasets used for this paper derive from the regional rain gauge network, managed by Hydrographic Service of Abruzzo Region: 72 stations have been selected for 2017 and 2018 as they were the only ones with complete monthly data for the considered period (Figure 1 and Table 1).

Furthermore, in the Abruzzo region there are four radar sensors installed, but only two of them converge into the national radar mosaic which is used in this study: *Mt. Il Monte* and *Mt. Midia* radars (pink triangles in Figure 1). Mosaicked data are processed to produce monthly and annual cumulative datasets of precipitation.

2.2. Geostatistical method

The Ordinary Kriging (OK) technique [8-9-11] was selected to spatialize rainfall data sampled at the gauging station of the Abruzzo Region monitoring network (Figure 1). In OK, the selected target variable ($z^*(\mathbf{x}_0)$) can be calculated at each location of a domain grid ($\mathbf{x}_0$) through an unbiased and optimal estimator, namely the Best Linear Unbiased Estimator (BLUE), described by the following equation:

$$z^*(\mathbf{x}_0) = \sum_{i=1}^{N} \lambda_i z(\mathbf{x}_i) \qquad \text{with } i = 1, \dots, N \tag{1}$$

In Eq. (1), λ_i are the weights attributed to the variable values ($z(\mathbf{x}_i)$) measured at specific locations in the neighborhood ($\mathbf{x}_i$).

BLUE ensures that the estimated values are the most optimal and unbiased (i.e., $E\left(z^*(\mathbf{x}_0) - z(\mathbf{x}_0)\right) = 0$) possible by imposing the following condition:

$$\sum_{i} \lambda_i = 1 \tag{2}$$

This constrain is included in the Kriging equation system (Eq. (3)), which consists of a set of $N + 1$ linear equations, as shown below:

$$\begin{cases} \sum_{j=1}^{N} \lambda_i \gamma(\mathbf{x}_i, \mathbf{x}_j) + \mu = \gamma(\mathbf{x}_i, \mathbf{x}_0) \\ \sum_{j=1}^{N} \lambda_j = 1 \end{cases} \tag{3}$$

where μ is a Lagrangian multiplier, whereas $\gamma(\mathbf{x}_i, \mathbf{x}_j)$ and $\gamma(\mathbf{x}_i, \mathbf{x}_0)$ are the semi-variograms (or variograms) related to pairs of measurements and to pairs that include the unsampled location ($\mathbf{x}_0$).

Preprints (www.preprints.org) | NOT PEER-REVIEWED | Posted: 2 November 2022 doi:10.20944/preprints202211.0051.v1

In geostatistics, the variogram is a function that describes the spatial dependency of a given random variable of interest [30] as a relation between semi-variance ($\gamma(\mathbf{h})$) and distance, described by a separation vector called lag ($\mathbf{h}$). Variograms are defined by the following equation (Eq. (4)):

$$\gamma(\mathbf{h}) = \frac{1}{N(\mathbf{h})} \sum_{i=1}^{N(\mathbf{h})} [z(\mathbf{x}_i) - z(\mathbf{x}_i + \mathbf{h})]^2 \qquad \text{with } i = 1, \dots, N(\mathbf{h}) \tag{4}$$

In this equation, $z(\mathbf{x}_i)$ and $z(\mathbf{x}_i + \mathbf{h})$ are a pair of distinct measurements separated by a lag $\mathbf{h}$ regarding a specific location within the considered domain ($\mathbf{x}_i$), while $N(\mathbf{h})$ is the number of pairs separated by the same lag.

To solve the linear equation system in Eq. (3), the experimental variogram (i.e., the one obtained from actual measurements) is fitted by a variogram model, which can be either simple e (i.e., one spatial structure) or nested (i.e., two or more spatial structures).

Besides the predicted value, OK provides a measure of the uncertainty associated with the estimate, namely the Kriging variance ($\sigma^2(\mathbf{x}_0)$), as follows:

$$\sigma^2(\mathbf{x}_0) = \mu + \sum_{i=1}^{N} \lambda_i \gamma(\mathbf{x}_i, \mathbf{x}_0) \tag{5}$$

Since in the case of variables characterized by a non-Gaussian statistical distribution the prediction may be non-linear and then not optimal, and the Kriging variance, or the corresponding standard deviation, cannot be used as a local measure of error [31]. For this reason, the yearly and monthly rainfall were transformed through a function well-known in geostatistics: the Gaussian Anamorphosis [10]. This function can convert a Gaussian variable ($Z = \Phi(Y)$) into a non-Gaussian one by fitting a polynomial expansion, as defined in Eq. (6):

$$\Phi(Y) = \sum \Psi_i H_i(Y) \tag{6}$$

where, $H_i(Y)$ are the Hermite polynomials, while Ψ_i are the Hermite coefficients.

Once defined, this function can be inverted and used to transform a non-Gaussian variable into a standardized one (Eq. (7)):

$$Y = \Phi^{-1}(Z) \tag{7}$$

In this study, raw rainfall data were previously transformed into standardized Gaussian variables and then interpolated. Finally, the predictions were back transformed to obtain the yearly and monthly rainfall maps with the origin unit through the Gaussian Anamorphosis function. Back-transformation was applied to 95% confidence interval limits (Lower Limit–LL, and Upper Limit–UL) maps as well, obtained by the following relation:

$$\text{Limits of 95\% CI} = z^*(\mathbf{x}) \pm \frac{1.96\sigma}{\sqrt{n}} \tag{8}$$

where, σ is the OK standard deviation, while n the optimal number of measurement locations in the neighborhood.

The performance of selected variogram models used in the OK analyses was evaluated using the cross-validation, which consist of sequentially removing the measurements one at a time and estimating each one of them at the corresponding sampling location, using the model under evaluation and the experimental data in the neighborhood. The differences between measured values and estimates represent errors, from which t is possible to calculate the following performance evaluation statistics, with their reference value:

Preprints (www.preprints.org) | NOT PEER-REVIEWED | Posted: 2 November 2022 doi:10.20944/preprints202211.0051.v1

$$\text{Mean Error} = \text{ME} = \frac{1}{N}\sum_{i=1}^{N}(z_i^* - z_i) \to 0 \quad (9)$$

$$\text{Mean Standardized Error} = \text{MSE} = \frac{1}{N}\sum_{i=1}^{N}\left(\frac{z_i^* - z_i}{\sigma_i}\right) \to 0 \quad (10)$$

$$\text{Root Mean Squared Error} = \text{RMSE} = \sqrt{\frac{1}{N}\sum_{i=1}^{N}(z_i^* - z_i)^2} \to 0 \quad (11)$$

$$\text{Root Mean Squared Standardized Error} = \text{RMSSE} = \sqrt{\frac{1}{N}\sum_{i=1}^{N}\left(\frac{z_i^* - z_i}{\sigma_i}\right)^2} \to 1 \quad (12)$$

In which, z_i^* and z_i are the estimated and measured values, N is the number of sampled locations, and σ_i is the Kriging standard deviation.

ME and MSE measure the variogram model unbiasedness, RMSE for its precision, whereas RMSSE for its accuracy.

The rainfall values were estimated by OK through Eq. (1) on the same grid (i.e., support) as the weather radar rasters (cell size of 1000-1000 m), to make the comparison reliable. Eventually, the output rasters were sliced into the four altimetric zones, rain data have been sampled from every pixel and the mean rainfall amount has been calculated for each zone.

All the geostatistics analyses were preformed using the software Geovariances Isatis.neo 2021.07 (www.geovariances.com/en/software/isatis-neo-geostatistics-software/)

2.3. Weather RaDAR method

Weather radar are active instruments that emits electromagnetic (EM) waves, typically in the microwave spectrum and, after the interaction of the EM signal sent with hydrometeors in the atmosphere, the reception of the backscattered component is used to infer some key geophysical information (e.g. hydrometeor typology like rain, hail, show, water content, rain rate, etc.). Single polarized radars allow the reception of the backscattered power in one single polarization, typically the horizontal one (h) to derive the reflectivity factor (Z_{hh}) which is strongly dependent to the six-power of the size of hydrometeors intercepted along the radar ray path. After a proper calibration and processing, Z_{hh} is converted into instantaneous surface rainfall intensity (S_R) expressed in (mm/h) using the following power law equation:

$$S_R = \left(10^{\frac{Z_{hh}}{10}}\right)^{\frac{1}{b}}\left(\frac{1}{a}\right)^{\frac{1}{b}} \quad (13)$$

where a and b are two dimensional coefficients geographically calibrated [13], and Z_{hh} is conventionally expressed in $mm^6\ m^{-3}$. S_R in then converted into hourly accumulation by assuming constant rain within the time elapsed between two consecutive radar acquisitions so that hourly precipitation (P_{1h}) is

$$P_{1h} = \sum_{t=1}^{N} S_R(t)\Delta t \quad (14)$$

Where Δt is the time sampling of the radar in (h) and N is the number of the radar acquisitions in the hour considered. Larger accumulation periods are obtained summing the needed number of hours. It is worth mentioning that dual polarized radars are multivariable systems adding more information on the shape and composition of hydrometeors

Preprints (www.preprints.org) | NOT PEER-REVIEWED | Posted: 2 November 2022 doi:10.20944/preprints202211.0051.v1

allowing to constrain Eq. (13) and obtain more accurate rain estimates [32]. In addition, these systems allow a better discrimination of the unwanted radar returns thus achieving a better data quality which also indirectly contribute to the accuracy of S_R [16].

The C-band weather radars data used in this work comes from the Italian mosaic for a 2017-2018 period with a temporal resolution of Δt =10 min and raster representation with a grid spacing if 1×1 km². For the Abruzzo territory, the main contributing radars are those of *Il Monte* (lon=14.621°, lat=41.939°, alt=710 m), and *Mt. Midia* radar (lon=13.177°, lat=42.057°, alt=1660 m) managed by the Italian civil protection and the regional authority, respectively. *Il Monte* radar is a Doppler dual polarized system, and it mostly covers the coastal eastern side, whereas *Mt. Midia* is a Doppler single polarized system, and it has an open view mainly in the westmost part of the region. Because of the different radar site altitudes, and polarization capability of *Il Monte* radar with respect to *Mt. Midia* one, that suggests a better data quality of the former than the latter, different rain retrieval performances are expected in the respective areas covered by the two radars.

Figure 2, illustrates, for reference only, the average monthly rain accumulation for March 2017 obtained by the radar mosaic for the Abruzzo region.

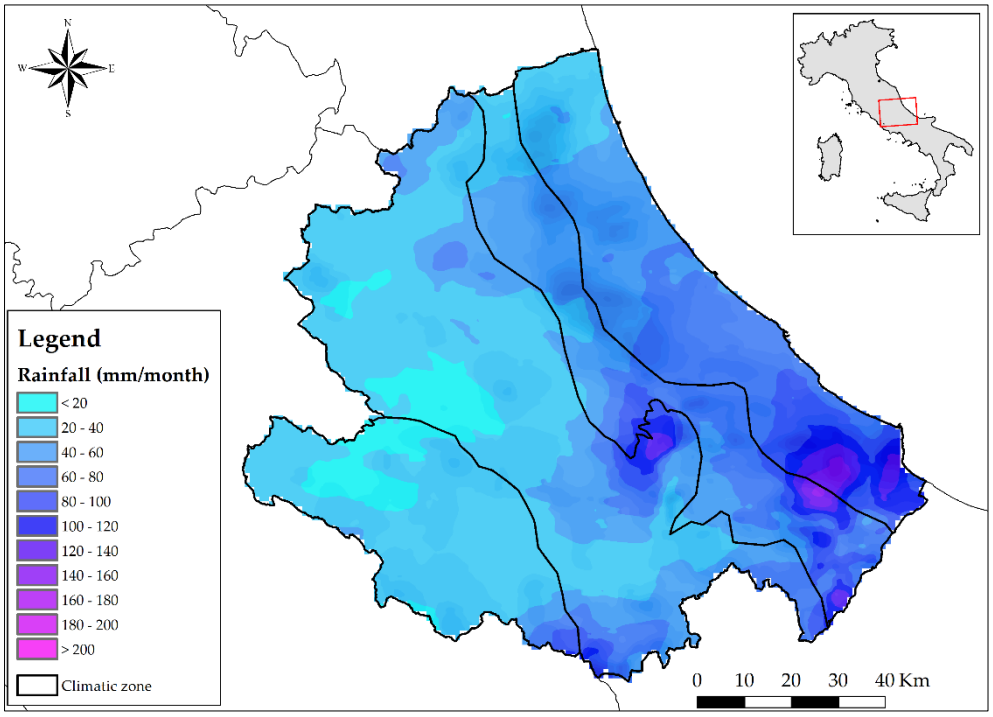

Figure 2. Raster map showing radar monthly cumulate for March 2017. Altimetric - climatic zone are displayed, too.

Radar data represented in the maps are processed at the central level with a composite technique that permits better territory coverage and rainfall quantification. As mentioned earlier some uncertainties can affect these data: orographic blocks, disturbing interferences, path attenuation fostered by strong precipitation [16]. Using a composite radar data and polarimetry, when available, these issues can be partially overcome. For orographic echoes (ground clutter), they are successfully removed using clutter maps (i.e. representation of static obstacles in the radar view geometry using statistic of clear sky radar acquisitions, [33] as well as polarimetric filters when available [12].

The radar dataset analyzed extends to two years. The limitation to only two years of analysis is justified by the huge amount of data to be processed and to the identification of complete monitoring periods of the meteorological stations. With respect to a few thousand of daily data from rain gauge, the weather radar analysis provides for the processing of tens millions of data for month. These records are cumulated to a monthly temporal

Preprints (www.preprints.org) | NOT PEER-REVIEWED | Posted: 2 November 2022 doi:10.20944/preprints202211.0051.v1

time frame and represented as raster monthly radar maps. Additional annual maps have been provided for both years.

3. Results and discussion

Rain data from gauging stations have been cumulated monthly and annually for 2017 and 2018 and then interpolated using the Ordinary Kriging (OK).

In Figure 3 and Table 2, as an example, annual fitted variogram models related to the gaussian-transformed rainfall data and their performace statistics from the cross-validation are shown, respectively.

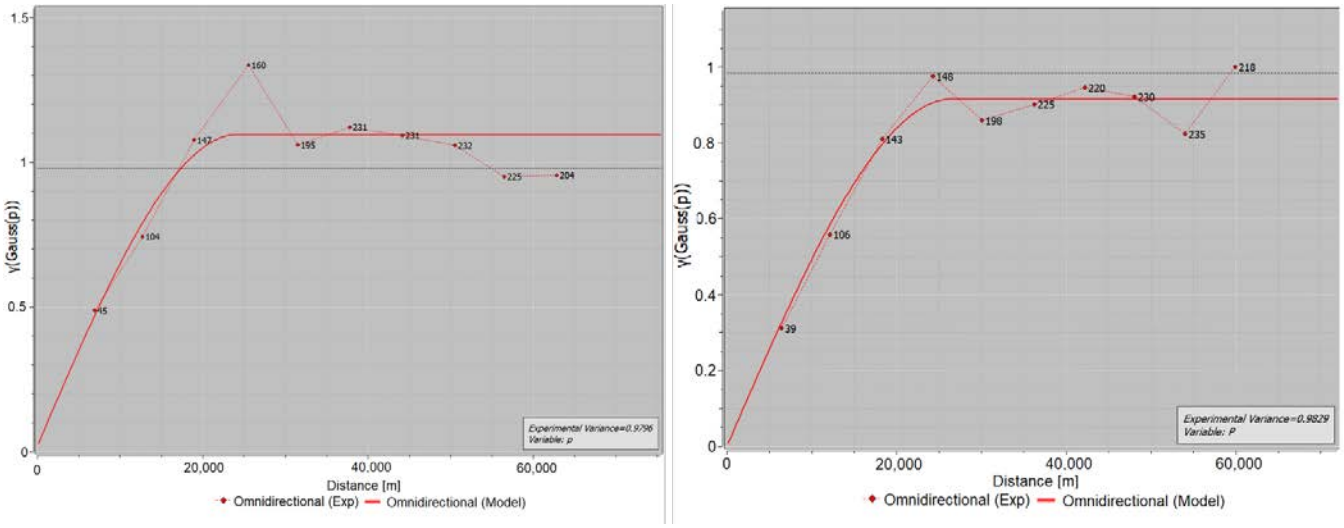

Figure 3. Variogram (variance vs. distance) examples. To the left: 2017; to the right: 2018.

Table 2. Cross-validation related to 2017 and 2018 variogram shown in Figure 3.

2017 cross-validation	
ME	0.00
MSE	-0.0029
RMSE	0.78
RMSSE	0.9518
2018 cross-validation	
ME	0.01
MSE	0.0087
RMSE	0.85
RMSSE	1.0553

For both annual datasets, a spherical variogram model was selected; for 2017, the range is equal to about 24200 m, while for 2018 the range is about 26600 m.

The selected variogram models reflect a satisfying level of unbiasedness, precision, and accuracy, as demonstrated by the cross-validation results.

As outputs, 13 raster maps for each year have been carried out. The same cumulation periods used for rain gauges is used for radar data.

All the obtained rasters are sliced in the four altimetric zones (Figure 1) as shown in Figure 4, where the comparison between OK interpolated data (left panels) and radar estimates (right panels) are represented for 2017 and 2018 (in the upper and lower panels, respectively).

Preprints (www.preprints.org) | NOT PEER-REVIEWED | Posted: 2 November 2022 doi:10.20944/preprints202211.0051.v1

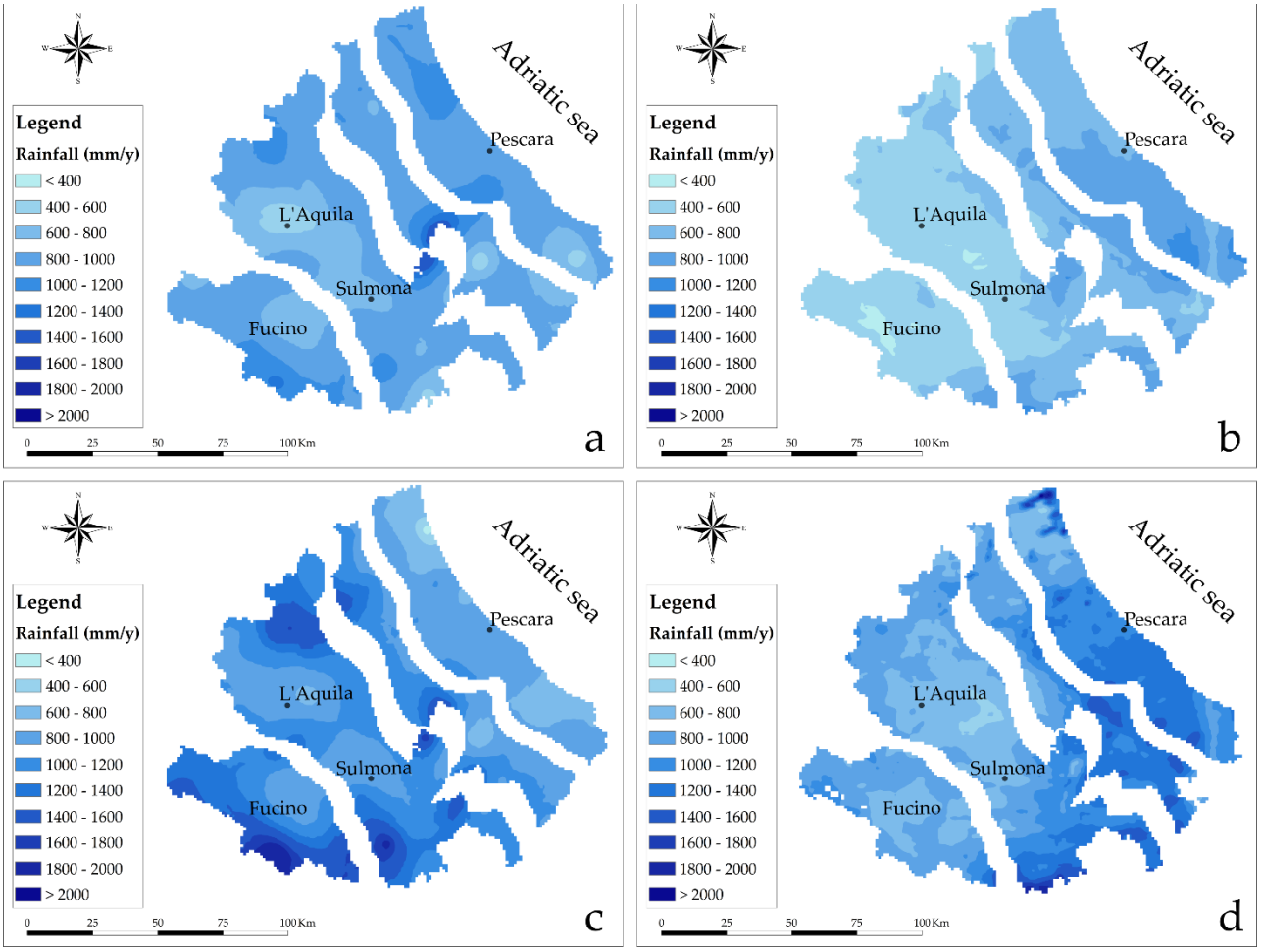

Figure 4. Comparison between OK interpolated data and weather radar ones using the raster maps sliced in the four zones: (**a**) 2017 OK interpolated data (**b**) 2017 weather radar data (**c**) 2018 OK interpolated data (**d**) 2018 weather radar data.

As can be seen in Figure 4a, where OK interpolated data for 2017 are displayed, spots of lower values are in the southern part of coastal and hilly areas, due to local minima in the rainfall measures from the rain gauge stations located in those zones. Likewise, a similar situation can be found in Sulmona, L'Aquila and Fucino plains where rainfall values are more modest than the surrounding ones. Generally, coastal, and hilly areas indicate the highest rainfall values.

The 2017 weather radar data are shown in Figure 4b, where is clear that coastal and hilly areas' rainfall values are higher than mountain and Marsica ones, confirming what deduced from OK interpolation with plain internal regions that are the less rainy.

The 2018 OK interpolated data (Figure 4c) show similar features to 2017: plains have the lower values, and the spots in the southern part of coastal and hilly areas; on the other hand, for 2018 mountain and Marsica zones are rainier than the other two, unlike 2017.

Weather radar data from 2018 (Figure 4d) have the same 2017 trend which indicates greater rain amount in coastal and hilly portions and lower ones in intramountain plain.

For a deeper and more accurate comparison between the two types of inflow estimations, the corresponding mean rainfall amounts (mm) have been considered and elaborated seasonally in each climatic area for every single month and summed as seasonal cotributions:

- January, February, and December as winter,
- March, April, and May as spring,
- June, July, and August as summer,
- September, October, and November as fall.

Preprints (www.preprints.org) | NOT PEER-REVIEWED | Posted: 2 November 2022 doi:10.20944/preprints202211.0051.v1

Using both types of data, weather radar and OK ones, monthly rainfall amounts have been summed up to obtain the quantities reported in Figure 5 where seasonal results are shown the two years analyzed.

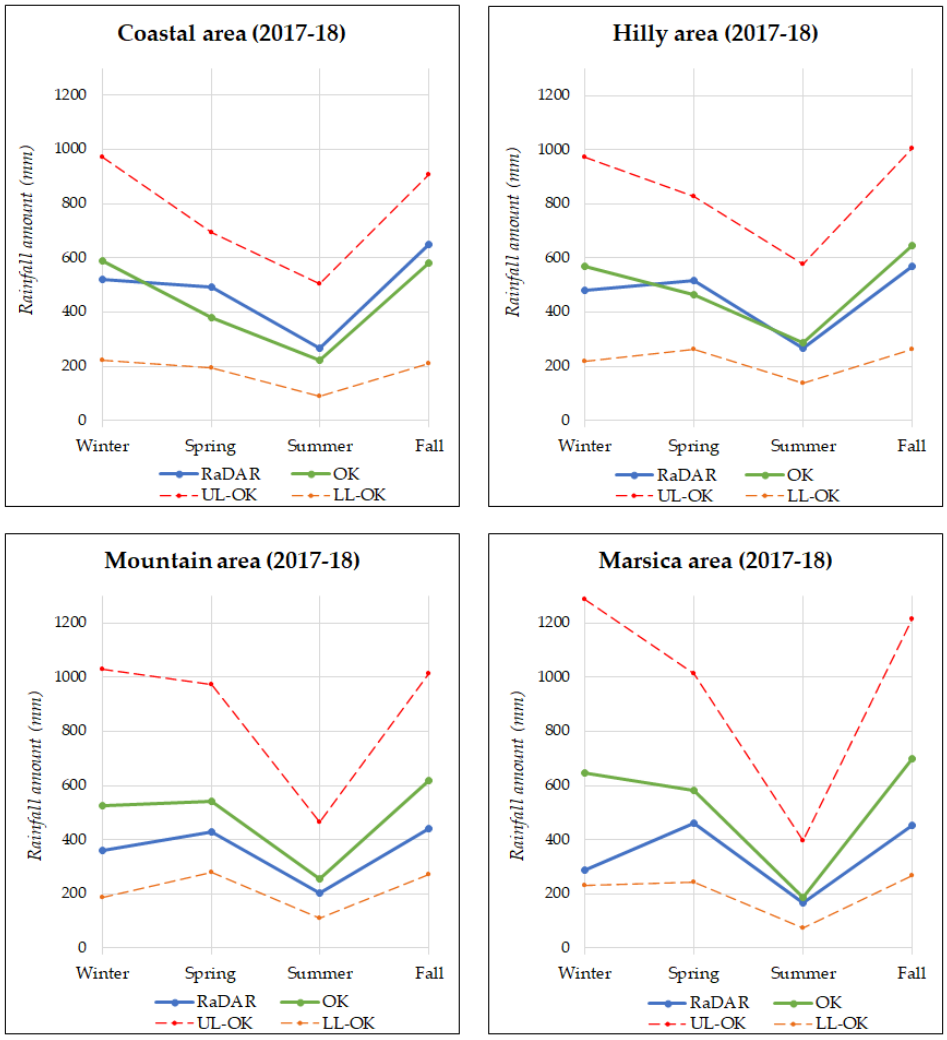

Figure 5. Rainfall amount (mm) for every altimetric area considering seasonal datasets for both radar and OK interpolated data (OK); Upper Limit (UL-OK) and Lower Limit (LL-OK) of the confidence interval are shown, as well.

As can be seen, all the graphs show higher values in OK interpolated data (OK in the graphs), except for coastal and hilly areas in which radar and OK tends to a better overall agreement. This can be explained by the fact that those area are mainly covered by the *Il Monte* radar which has the advantage of polarimetry and it is positioned closer the sea level thus having a closer agreement with ground stations.

The highest discrepancies are shown for winter and fall rainfall amounts, especially in mountain and Marsica areas whereas the best correspondence is for summer data in all the four zones. One possible explanation to this behavior can be attributed to the fact that in the summer the freezing level altitude is higher than in the winter and, consequently, in the summer radar observations are performed in rain regime (i.e. they are likely picked up at altitudes below the freezing level). Contrarily, in the winter, the radar is more likely sampling in ice/snow regimes, especially when the freezing level is approaching the radar site altitude (i.e. 1660 m). Thus, as evidenced in Figure 5, in the summer we expect an augmented consistency between the radar estimated and rain gauges, as the two sources

Preprints (www.preprints.org) | NOT PEER-REVIEWED | Posted: 2 November 2022 doi:10.20944/preprints202211.0051.v1

both sample rain. In this context, *Mt. Midia* radar positioned at 1660 m of altitude is disadvantage during the winter thus contributing significantly to the errors registered in the mountain and Marsica areas during fall and winter periods.

As highlighted in Figure 5, the mountain and Marsica zones shows the greatest differences in seasonal comparison; at the same time, these two are the poorest in terms of rain gauge stations and weather radar could represent a good solution. For these reasons and for a deeper investigation, rainfall data and the altitudes corresponding with the gauging stations' locations have been correlated.

In any case, seasonal rainfall amount estimated from RaDAR data always fall into the 95% confidence interval of the OK estimates, which means that they are able to catch the spatial and temporal variability in an acceptable way, and little efforts (e.g., bias correction in the post-processing phese) is required to make them reliable for quantitative purposes.

Figure 6 points out this relationship for the two years period considered. Rainfall data are from gauging stations located in mountain and Marsica areas and cumulated annually; weather radar data have been extracted from annual raster maps at the locations corresponding to the positions of the rain gauge stations within each area considered. Both these rainfall datasets have been correlated with automatic stations altitudes.

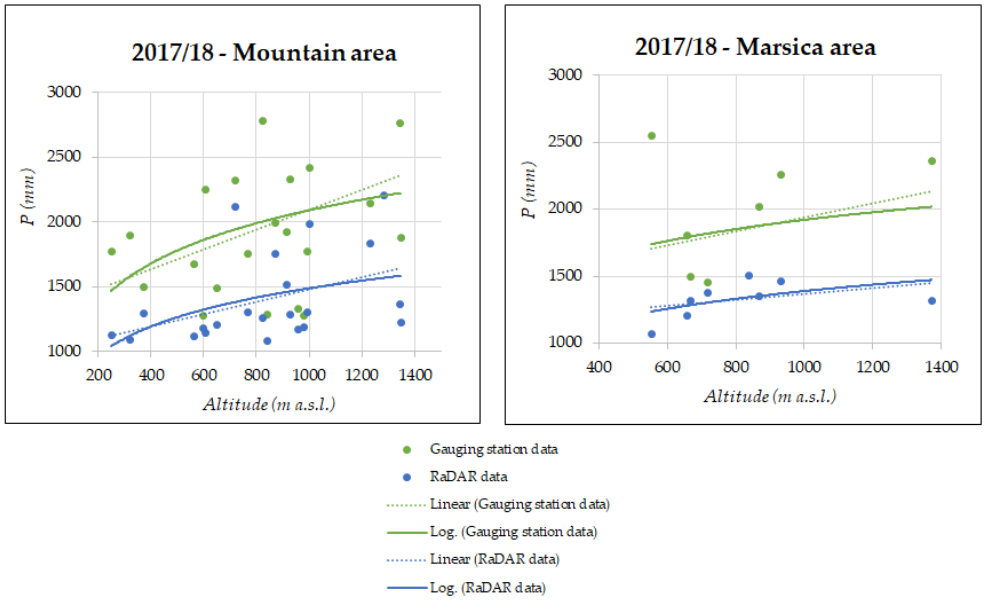

Figure 6. Correlation altitude/precipitation (P) using rainfall data from gauging stations and weather radar datasets in mountain and Marsica areas for 2017-2018 years. *Linear* and *Log.* indicate regression lines.

As can be seen, data from gauging stations are more "scattered" than weather radar ones, especially in Marsica area; consequently, these dispersed distributions do not allow to deduce a clear rainfall-altitude correlation.

Despite these issues both linear and logarithmic regressions have been tried out finding that linear correlation fits better than logarithmic one.

These diagrams confirm the higher values in gauging stations' datasets as already seen in Figure 5 and more importantly, they come up with a way to correct radar estimates in complex orography or wide areas [20]. Indeed, it seems that the differences (bias) that characterize the two curves (dotted blue and green one) in Figure 5 are almost parallel to each other thus suggesting that the bias found at lower altitude is applicable to higher ones. This finding could be a first aid for a radar estimates bias correction in pre-selected complex orography environments, namely, datasets collected in more denser areas at lower altitudes can be used to extrapolate the found bias at higher, and less instrumented, altitude areas. Hydrological applications can particularly benefit from such bias correction being them mainly sensible to forcing input at the basin upstream.

 doi:10.20944/preprints202211.0051.v1

4. Conclusions

Although weather radars are widely used as ground reference in many hydro-meteorological applications, the elaborations performed in this study, verified as their rain estimates, especially in an operational context, can suffer of non-negligible errors, if compared with rain gauge networks. Thus, rain gauges and weather radars appear to be integrative with each other and in particular the former can cooperate with the latter to compensate, at least on average, for some retrieval biases. The radar and rain gauge comparison performed in the Abruzzo region highlighted the following positive aspects:

- good agreement between the two sources in the warmer seasons due to the homogeneity in the quantity observed by the radar and rain gauges;
- general good agreement in the coastal and hilly areas due to the better radar coverage in those area of one of the two radars used in the analysis. This also suggest the importance of studying the radar view geometry compared to the local orography to identify areas where better results are expected.

Among the problematic aspects that require further study, we highlight:

- general underestimation of the results obtained by weather radar. Although the radar underestimation is very well known, its compensation can be less obvious in complex orography as pointed out in this work. The selection of homogenous climatic and altitude areas, as suggested in this study, could be a way out to compensate for the radar underestimation problem,
- worse agreement between the radar and rain gauges in the cold and rainy seasons (especially in winter and autumn in the Mountain and high plains areas) which is justified by the mismatch in the observation of the same precipitation regime by the radar and rain gauge. Such a problem is more severe when the altitude of the radar site is closer to the altitude of the freezing level because in such situation the radar likely observes ice/snow whereas rain gauges catch liquid water.

Considering the discrepancies in the results obtained with the two measuring methods, weather radar needs to be better elaborated, compensating biases in order to fill the lack of directly measure inflows at high altitude where gauging stations are not present. To this end, future works will investigate the possibility to use the knowledge of hydrogeological balance in well-known aquifer and catchment areas where the hydrometeor inflow can also be calculated by the sum of the water outlets and evapotranspiration.

Author Contributions: Conceptualization, SR, ADG, DDC and MM; collection of data, DDC, ADG, RL; data processing, ADG, DDC, RL; interpretation of results, SR, DDC, ADG, MM, RL; writing-original draft preparation, ADG, DDC, MM, SR; writing-review and editing, SR, ADG, DDC, MM, RL; supervision, SR. All authors have read and agreed to the published version of the manuscript.

Funding: This research received no external funding.

Institutional Review Board Statement: Not applicable.

Informed Consent Statement: Not applicable.

Conflicts of Interest: The authors declare no conflict of interest.

References

[1] Chiaudani, A.; Di Curzio, D.; Rusi, S. The snow and rainfall impact on the Verde spring behavior: A statistical approach on hydrodynamic and hydrochemical daily time-series. *Sci. of the Tot. Envir.* **2019**, 689, 481-493. https://doi.org/10.1016/j.scitotenv.2019.06.433

[2] Fronzi, D.; Di Curzio, D.; Rusi, S.; Valigi, D.; Tazioli, A.; Comparison between periodic tracer tests and time-series analysis to assess mid-and long-term recharge model changes due to multiple strong seismic events in carbonate aquifers. *Water* **2020**, 12(11). https://doi.org/10.3390/w12113073

[3] Navarro, A.; García-Ortega, E.; Merino, A.; Sánchez J. L.; Tapiador F. J. Orographic biases in IMERG precipitation estimates in the Ebro River basin (Spain): The effects of rain gauge density and altitude. *Atm. Res.* **2020**, 244, 105068. https://doi.org/10.1016/j.atmosres.2020.105068.

[4] Di Curzio, D.; Rusi, S.; Di Giovanni, A.; Ferretti, E. Evaluation of Groundwater Resources in Minor Plio-Pleistocene Arenaceous Aquifers in Central Italy. **Hydrology 2021**, **8**, 121. https://doi.org/10.3390/hydrology8030121.
[5] Thiessen, A.H.; Precipitation average for large areas. *Mon. weat. rev.* **1911**.
[6] Lyra, G.B.; Correia, T.P.; de Oliveira-Júnior, J.F.; Zeri, M.; Evaluation of methods of spatial interpolation for monthly rainfall data over the state of Rio de Janeiro, Brazil. *The. and App. Clim.* **2018**, 134(3), 955-965. https://doi.org/10.1007/s00704-017-2322-3.
[7] Matheron, G. The intrinsic random functions and their applications. *Adv. in Appl. Prob*. **1973**, 5, 439–468.
[8] Journel, A.G.; *Fundamentals of geostatistics in five lessons (Vol. 8).* American Geophysical Union: Washington, D.C., USA, 1989. https://doi.org/10.1002/9781118667606.ch0
[9] Webster, R.; Oliver, M.A. *Geostatistics for Environmental Scientists*. John Wiley & Sons: New York, USA, 2007. https://doi.org/10.1002/9780470517277
[10] Chilès J.-P.; Delfiner P. *Geostatistics: Modeling Spatial Uncertainty*, 2nd ed.; Wiley: Hoboken, NJ, USA, 2012.
[11] Castrignanò; A., *Introduction to Spatial Data Processing* Aracne: Rome, Italy, 2011.
[12] Barbieri, S.; Di Fabio, S.; Lidori, R.; Rossi, F.L.; Marzano, F.S.; Picciotti, E. Mosaicking Weather Radar Retrievals from an Operational Heterogeneous Network at C and X Band for Precipitation Monitoring in Italian Central Apennines. *Rem. Sens.* **2022**, 14, 248. https://doi.org/10.3390/rs14020248.
[13] Falconi, M.T.; Marzano, F.S. Weather Radar Data Processing and Atmospheric Applications: An overview of tools for monitoring clouds and detecting wind shear. *IEEE Sig. Proc. Mag.* **2019**, 36 85-97. https://doi.org/10.1109/MSP.2019.2890934.
[14] Montopoli, M.; Roberto, N.; Adirosi, E.; Gorgucci, E.; Baldini, L. Investigation of Weather Radar Quantitative Precipitation Estimation Methodologies in Complex Orography. *Atm.* **2017**, 8, 34. doi:10.3390/atmos8020034.
[15] Germann, U.; Boscacci, M.; Clementi, L.; Gabella, M.; Hering, A.; Sartori, M.; Sideris, I.V.; Calpini, B. Weather Radar in Complex Orography. *Rem. Sens.* **2022**, 14, 503. https://doi.org/10.3390/rs14030503.
[16] Vulpiani, G.; Montopoli, M.; Delli Passeri, L.; Gioia, A. G., Giordano, P.; Marzano, F.S. On the use of dual-polarized C-band RaDAR for operational rainfall retrieval in mountainous areas, *J. Appl. Meteor. Climat*. **2012**, 51 (2), 405-425. https://doi.org/10.1175/JAMC-D-10-05024.1.
[17] Federico, S.; Torcasio, R. C.; Avolio, E.; Caumont, O.; Montopoli, M.; Baldini, L.; Vulpiani, G.; and Dietrich, S. The impact of lightning and radar reflectivity factor data assimilation on the very short-term rainfall forecasts of RAMS@ISAC: application to two case studies in Italy, *Nat. Haz. Ear. Syst. Sci*. **2019**, 19, 1839–1864. https://doi.org/10.5194/nhess-19-1839-2019.
[18] Montopoli, M.; Picciotti, E.; Baldini, L.; Di Fabio, S.; Marzano, F.S.; Vulpiani, G. Gazing inside a giant-hail-bearing Mediterranean supercell by dual-polarization Doppler weather RaDAR. *Atm. Res.* **2021**, 264, 105852. https://doi.org/10.1016/j.atmosres.2021.105852.
[19] Di Curzio, D.; Di Giovanni, A.; Lidori, R.; Marzano, F. S.; Rusi, S. Investigating the feasibility of using precipitation measurements from weather RaDAR to estimate potential recharge in regional aquifers: the Majella massif case study in Central Italy. *Acq. Sott. – Ital. J. of Groun.* **2022**, 11(3). 41–51. https://doi.org/10.7343/as-2022-568.
[20] Areerachakul, N.; Prongnuch, S.; Longsomboon, P.; Kandasamy, J. Quantitative Precipitation Estimation (QPE) Rainfall from Meteorology Radar over Chi Basin. *Hydrology* **2022**, 9, 178. https://doi.org/10.3390/hydrology9100178
[21] Sollitto, D.; Romic, M.; Castrignanò, A.; Romic, D.; Bakic, H.; Assessing heavy metal contamination in soils of the Zagreb region (Northwest Croatia) using multivariate geostatistics. *Catena* **2010**, 80(3), 182-194. https://doi.org/10.1016/j.catena.2009.11.005
[22] Di Curzio D., Rusi S., Signanini P. Advanced redox zonation of the San Pedro Sula alluvial aquifer (Honduras) using data fusion and multivariate geostatistics. *Sci. of the Tot. Envir*. **2019**, 695, 133796. https://doi.org/10.1016/j.scitotenv.2019.133796.
[23] Manzione, R.L.; Castrignanò, A.; A geostatistical approach for multi-source data fusion to predict water table depth. *Sci. of the Tot. Envir*. **2019**, 696, 133763. https://doi.org/10.1016/j.scitotenv.2019.133763
[24] Vessia, G.; Di Curzio, D.; Chiaudani, A., Rusi, S.; Regional rainfall threshold maps drawn through multivariate geostatistical techniques for shallow landslide hazard zonation. *Sci. Total Environ.* **2020**, 705, 135815 https://doi.org/10.1016/j.scitotenv.2019.135815.
[25] Rivoirard, J.; On the structural link between variables in kriging with external drift. *Mathematical geology* **2002**, 34(7), 797-808. https://doi.org/10.1023/A:1020972510120
[26] Hengl, T.; Geuvelink, G.B.M.; Stein, A. Comparison of kriging with external drift and regression-kriging. Technical note, ITC, The Netherlands, 2003. Available on-line at http://www.itc.nl/library/Academic output.
[27] Buttafuoco, G.; Conforti, M. Improving Mean Annual Precipitation Prediction Incorporating Elevation and Taking into Account Support Size. *Water* **2021,** 13(6), 830. https://doi.org/10.3390/w13060830.
[28] Vergni, L.; Di Lena, B.; Chiaudani, A. Statistical characterisation of winter precipitation in the Abruzzo region (Italy) in relation to the North Atlantic Oscillation (NAO). *Atmospheric Research* **2016**, 178-179, 279-290. https://doi.org/10.1016/j.atmosres.2016.03.028.
[29] Vergni, L.; Todisco, F.; Di Lena, B.; Mannocchi F. Effect of the North Atlantic Oscillation on winter daily rainfall and runoff in the Abruzzo region (Central Italy). *Stoch Environ Res Risk Assess* **2016**, 30, 1901–1915. https://doi.org/10.1007/s00477-015-1194-2.
[30] Vessia, G.; Di Curzio, D.; Castrignanò, A. Modeling 3D soil lithotypes variability through geostatistical data fusion of CPT parameters. *Sci. of the Tot. Envir*. **2020**, 698, 134340. https://doi.org/10.1016/j.scitotenv.2019.134340.
[31] Goovaerts, P. Geostatistics for natural resources evaluation. Oxford University Press, 1997.

[32] Adirosi, E.; Roberto, N.; Montopoli, M.; Gorgucci, E.; Baldini, L. Influence of Disdrometer Type on Weather Radar Algorithms from Measured DSD: Application to Italian Climatology. *Atmosphere* **2018**, 9, 360. https://doi.org/10.3390/atmos9090360

[33] Harrison DL, Driscoll SJ, Kitchen M (2000) Improving precipitation estimates from weather radar using quality control and correction techniques. *Meteorol. Appl.* **2000**, 7: 135-144. https://doi.org/10.1017/s1350482700001468.